A Distributed Medium Access Control Scheme for a Large Network of Wireless Routers

Bin Zhao and Yingbo Hua, *Fellow, IEEE*

***Abstract*— The throughput of a large network of wireless routers critically depends on the design of distributed medium access control (MAC). In this paper, a distributed MAC scheme called opportunistic synchronous array method (SAM) is presented and analyzed. The opportunistic SAM combines multiuser diversity and interference suppression in a distributed fashion. Depending on the choice of two control parameters, the opportunistic SAM may reduce to three specializations: multiuser SAM, switching SAM or deterministic SAM. The network throughput of the opportunistic SAM is analyzed, and its throughput gain over its specializations is illustrated.**

***Index Terms*— Large network of wireless routers, medium access control, synchronous array method, network throughput.**

I. Introduction

THERE are situations where the mobility of an entire communication infrastructure is desirable. A large mobile communication infrastructure inevitably involves a large network of wireless routers. Each wireless router can serve as a virtual base station for many conventional mobile clients. To reduce networking and routing overheads, wireless routers can be designed to be much less mobile than mobile clients. A network of wireless routers is also called a mesh network, which corresponds to the second tier of a three-tier architecture of large ad hoc networks [1]. In this paper, we will focus on the mesh network, ignoring the mobile clients (the first tier) and the possible backbone access points (the third tier). The routers in the mesh network will also be referred to as nodes in this paper. We are interested in intra-network traffic, which is different from inter-network traffic via backbone access points.

The maximum per-node throughout of a large network of wireless routers is important especially when the network is heavily loaded. It has been argued that the maximum per-node throughput in bits-hops/s/Hz/node of a large network is upper bounded by a finite number as the number of nodes in the network increases [1], [2], [3] and [4]. The throughput unit bits-hops/s/Hz/node measures the number of bits times the number of hops travelled by the bits per second per Hertz from each source node. Note that each node in the network may act as both a source node (that transmits its own data) and a relay node (that relays data for other nodes). This throughput unit is fundamentally important since the maximal achievable value c in this unit does not depend on the node density nor the number of hops between a source node and its destination node. This value also corresponds to the pre-constant of the transport capacity in bits-meters/s/Hz/node of a large network in a unit disk [2]. Yet, the value c critically depends on the design of medium access control (MAC) schemes in addition to the properties of antennas and the conditions of wireless channels. In this paper, we present some of our efforts in searching for the best MAC scheme to maximize the value c.

In [5], the throughput of a large network based on a MAC scheme called ALOHA was analyzed. In [1], a MAC scheme called synchronous array method (SAM) was proposed and analyzed. The SAM has been shown to yield a much higher throughput than ALOHA for both omni-directional antennas and directional antennas [1], [6], [7]. Although applicable to fading channels, the SAM shown in [1] does not exploit the channel state information (CSI) of fading channels. The SAM in [1] will be referred to as deterministic SAM.

Channel fading is known to be a useful resource that can be opportunistically exploited for traffic scheduling in cellular networks. In [8] and [9], the CSI of all mobile users is exploited at a central base station through user selection and power control. In [10] and [11], the CSI of mobile users is exploited in a decentralized fashion through a MAC scheme called channel aware ALOHA. The channel aware ALOHA combines random access with a probabilistic traffic controller that maps CSI into a transmission probability. It is shown in [11] that the performance loss of the decentralized scheme, compared to its centralized counterpart, is only fractional.

In this paper, we introduce a distributed MAC scheme for a large network of wireless routers without any central processor. This scheme will be called opportunistic synchronous array method. The opportunistic SAM integrates the channel-aware opportunistic approach into the deterministic SAM. Yet, our work is different from [8], [9], [10], [11] in that their studies focus on cellular networks where co-channel interferences from adjacent cells is lumped into a noise term of fixed variance while ours is in the context of a large-scale multi-hop network where co-channel interferences cannot be treated as noise of fixed variance. Like the channel aware ALOHA, the opportunistic SAM employs a probabilistic control function to reduce co-channel interference in a decentralized fashion. It will be shown that the optimal probabilistic control function

Manuscript received August 21, 2006; revised March 30, 2007 and February 25, 2008; accepted March 21, 2008. The associate editor coordinating the review of this letter and approving it for publication was D. Zeghlache. This work was supported in part by the U. S. National Science Foundation under Grants No. ECS-0401310 and TF-0514736, the U. S. Army Research Laboratory under the Collaborative Technology Alliance Program, and the U. S. Army Research Office under the MURI Grant No. W911NF-04-1-0224. The U. S. Government is authorized to reproduce and distribute reprints for Government purposes notwithstanding any copyright notation thereon.

B. Zhao was with the Department of Electrical Engineering, University of California, Riverside, CA 92521. He is now with Cinea, Inc., 16 S. 17th Street, Richmond, VA 23219 (e-mail: zb34111@yahoo.com).

Y. Hua is with the Department of Electrical Engineering, University of California, Riverside, CA 92521 (e-mail: yhua@ee.ucr.edu).

Digital Object Identifier 10.1109/TWC.2008.060617.

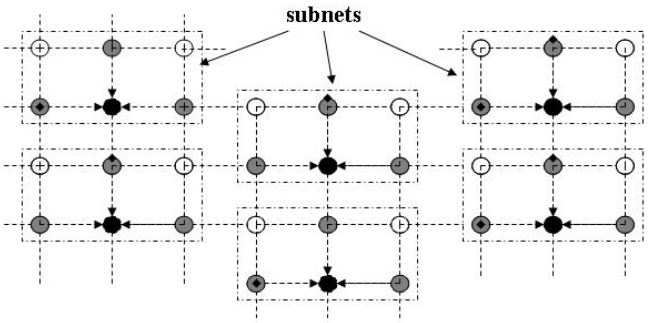

Fig. 1. A large network on square grid which is partitioned into subnets during a time slot of the synchronous array method (SAM). The black nodes denote the center (receiving) nodes, the gray nodes active neighboring nodes, and the white nodes idle neighboring nodes. Here, the center nodes are separated from each other with vertical spacing $p = 2$ and horizontal spacing $q = 3$.

is simply a step function. An important part of this paper is an analysis of the network throughput of the opportunistic SAM. Our analysis and numerical results demonstrate a significant improvement in network throughput of the opportunistic SAM over its specializations.

The rest of the paper is organized as follows. Section II describes the network model. Section III introduces the opportunistic SAM and its three specializations: multiuser SAM, switching SAM and deterministic SAM. Also shown in section III is the throughput analysis of the opportunistic SAM. Section IV illustrates the throughput of the opportunistic SAM for a large network of wireless routers located on a square grid. The final conclusion is provided in section V.

II. Network Model Under SAM

Consider a large network of wireless routers where time is slotted with equal duration. During each time slot, the entire network is virtually partitioned into $S + 1$ disjoint subnets $\{\mathcal{C}_j\}_{j=0}^{S}$. Each subnet $\mathcal{C}_j$ contains a center (receiving) node $\mathcal{Z}_j^0$, n_j active neighboring (potentially transmitting) nodes $\left\{\mathcal{Z}_j^i, 1 \le i \le n_j\right\}$, and m_j idle nodes.

Fig. 1 shows an example of a large network on a square grid where the black disks denote the center nodes, the gray disks the active neighbors, and the white disks the idle neighbors. In this example, each subnet is identical with $n_j = 3$ and $m_j = 2$. The center nodes are separated from each other with vertical spacing $p = 2$ and horizontal spacing $q = 3$. For different time slots, the pattern of the subnets is the same except for a relative relocation of the center nodes. With $p = 2$ and $q = 3$, it takes (at least) 6 time slots for each node on the network to become a center node.

During each time slot, the MAC scheme, opportunistic SAM, is applied at each subnet, where only one packet is possibly scheduled for transmission from one of the active neighbors to their center node. The details of the opportunistic SAM will be given in section III.

The channel between two arbitrary nodes is modeled as a single input and single output channel. The channel coefficient experiences a large scale path-loss and a small scale Rayleigh fading. The signal y_0 received by the center node in the subnet $\mathcal{C}_0$ can be expressed as

$$y_0 = \sum_{j=0}^{S} h_{0,j} x_j + w_0 \tag{1}$$

Here, x_0 is transmitted from one of the active neighbors in $\mathcal{C}_0$ which is the desired signal component for y_0, and x_j for $j \neq 0$ is transmitted from $\mathcal{C}_j$ for $j \neq 0$ which is the interference for y_0. The term w_0 denotes white Gaussian noise with zero mean and variance σ^2. The factor $h_{0,j}$ is the channel coefficient between the transmitter in $\mathcal{C}_j$ and the receiver in $\mathcal{C}_0$, which is assumed to be complex Gaussian with zero mean and the variance $E[|h_{0,j}|^2] = d_{0,j}^{-\alpha}$ where α is the path loss exponent and $d_{0,j}$ the distance between the transmitter in $\mathcal{C}_j$ and the receiver in $\mathcal{C}_0$. For convenience of throughput analysis, we assume that all transmitting nodes transmit with the same power P, i.e. $E\{|x_j|^2\} = P$ although this assumption is not necessary for the scheme.

Given (1), the instantaneous signal to interference and noise ratio (SINR) at the receiver in $\mathcal{C}_0$ is

$$SINR = \frac{\nu_{0,0} P}{\sigma^2 + \sum_{j \neq 0} \nu_{0,j} P} \tag{2}$$

where $\nu_{0,0} = |h_{0,0}|^2$ and $\nu_{0,j} = |h_{0,j}|^2$, which will also be referred to as channel gains. Unlike a cellular network problem, successive interference cancellation is difficult (if not impossible) to apply here, and thus all interferences are treated like noise. The instantaneous SINR at the receiver in $\mathcal{C}_0$ in a large network is generally unknown at the (desired) transmitter in $\mathcal{C}_0$. But we assume that the CSI in a local neighborhood (i.e. the channel gain $\nu_{0,0} = |h_{0,0}|^2$ between a center node and each of its neighbors) is available locally.

It then follows that the throughput of a large network in bits-hops/s/Hz/node is

$$c = \frac{1}{L} R_\xi P_d \tag{3}$$

where R_ξ is the packet spectral efficiency in bits/s/Hz with the (ideal) detection SINR threshold $\xi = 2^{R_\xi} - 1$, and $P_d = Pr\{SINR \ge \xi\}$ is the packet delivery probability, and $L = n_j + m_j + 1$ is the number of nodes in each subnet. (For convenience of computing the throughput, we will assume that n_j and m_j are independent of j unless specified otherwise.) Strictly speaking, the throughput (3) measures the throughput of nodes in the center of the network, which is a lower bound of the throughput of the entire network. But when the network is very large, almost all of the nodes experience the same level of interference as the nodes in the center of the network, and hence (3) is a valid network throughput.

Different MAC schemes affect differently the distribution of SINR and hence the throughput c. In the next section, we introduce the opportunistic SAM.

III. Opportunistic SAM

For the deterministic SAM [1], a pre-determined neighbor is scheduled to transmit a packet to the center node in each subnet during each time slot. This scheme is suitable when the channel state information (CSI) of each subnet is not available. But if the CSI of each subnet is available to some or all of the

nodes in the subnet, an opportunistic scheduling can be applied to select the best transmitter in each subnet during each time slot. Furthermore, if the channel gain of the best transmitter in a subnet is still not large enough, then the transmission in the subnet during that time slot can be aborted to reduce the interference to other subnets.

A. The Scheme

We now describe the details of the MAC scheme: opportunistic SAM. For convenience, we will refer to the subnet $\mathcal{C}_0$. Let the chosen transmitter in $\mathcal{C}_0$ be indexed by k_0. Then, k_0 is determined by

$$k_0 = \begin{cases} i_{max} & \text{with probability } s\left(\nu_{0,0}(i_{max})\right) \\ \{\phi\} & \text{with probability } 1 - s\left(\nu_{0,0}(i_{max})\right) \end{cases} \quad (4)$$

where $i_{max} = \arg\max_i \{\nu_{0,0}(i), 1 \le i \le n\}$, $\nu_{0,0}(i) = |h_{0,0}(i)|^2$ denotes the channel gain between the center node and its i^{th} neighbor, $\{\phi\}$ an empty set, and $s(\nu(i_{max}))$ maps the channel gain $\nu_{0,0}(i_{max})$ to a transmission probability with $0 \le s(\nu_{0,0}(i_{max})) \le 1$. According to (4), the opportunistic SAM first chooses a potential transmitter that has the largest channel gain and then probabilistically schedules a transmission for that transmitter with the probability $s(\nu_{0,0}(i_{max}))$.

In practice, to ensure a fairness, one can define $\nu_{0,0}(i) = f_i|h_{0,0}(i)|^2$ where f_i is a fairness factor to be decided for specific applications. For example, one can choose $f_i = \frac{a_i}{a_i+b_i}$ where a_i is the amount of data waiting to be transmitted from node i within the next time window T_a and b_i is the amount of data that have been transmitted from node i within the previous time window T_b. Both T_a and T_b should be application dependent. For throughput analysis, we will only consider the case where a_i dominates b_i such that $f_i = 1$.

Given (4), the duty cycle p of each subnet can be found as

$$p = \int_0^\infty s(x) f_{\nu_{\max}}(x) dx \quad (5)$$

where $\nu_{\max} = \nu(i_{max}) = \max_i \{\nu(i), 1 \le i \le n\}$, and $f_{\nu_{\max}}(x)$ denotes the probability density function (p.d.f.) of $\nu_{\max}$. The opportunistic SAM exploits a multiuser diversity when $n > 1$, and an interference suppression when $s(\bullet) \neq 1$.

In section III-C, we will prove that given a duty cycle p, the optimal form of $s(\bullet)$ is a step function, i.e. $s(x) = U(x - \theta)$ with $p = \int_\theta^\infty f_{\nu_{\max}}(x)dx$. Therefore, the opportunistic SAM for the subnet $\mathcal{C}_0$ can be further expressed as

$$k_0 = \begin{cases} i_{max} & \text{if } \nu_{0,0}(i_{max}) \ge \theta \\ \{\phi\} & \text{otherwise} \end{cases} \quad (6)$$

where $i_{max} = \arg\max_i \{\nu_{0,0}(i), 1 \le i \le n\}$. This scheme says that if and only if the largest channel gain for a subnet is larger than a threshold, there is a transmission in that subnet. Notice that the threshold θ can be different for different subnet although we will be interested to examine the throughput of a homogenous network for which θ is invariant from subnet to subnet.

It is clear that any abortion of transmission in a subnet reduces its interference to other subnets. Raising the threshold θ in each subnet reduces the total network co-channel interference. However it does not necessarily improve the network throughput since the average duty cycle p of each subnet is also reduced. One way to compensate such a throughput loss is to adjust the packet spectral efficiency R_ξ. In general, both the packet detection threshold ξ and the packet transmission threshold θ affect the network throughput. The optimal combinations of ξ and θ depend on various factors including the network topology and the channel fading statistics. In section IV, we will discuss the optimal combinations of ξ and θ for a large network on the square grid with block Rayleigh fading.

Before closing this subsection, we introduce three specializations of the opportunistic SAM:

- Multiuser SAM where $n > 1$ and $\theta = 0$. It only exploits "multi-user" spatial diversity in the subnet.
- Switching SAM where $n = 1$ and $\theta > 0$. It only exploits interference suppression.
- Deterministic SAM where $n = 1$ and $\theta = 0$. It is an extreme case of the opportunistic SAM where neither multiuser diversity nor interference suppression is exploited.

B. Channel Estimation

For the opportunistic SAM, the estimation of the channel gains $\{\nu(i), 1 \le i \le n\}$ within each subnet and each time slot is required. For the opportunistic SAM to be beneficial, this overhead measured in time must be much smaller than each time slot. Naturally, the coherence time of the channel gains must be no less than each time slot for data transmission.

The channel estimation of a large network requires a proper scheduling as well. Because of mutual interference between subnets, there should be sufficient distances between concurrent co-channel transmitters of training packets. Assume that it takes g cycles of channel training for each subnet to obtain a single channel estimation. Since each subnet has n potential transmitters, we need ng cycles of channel training. Clearly, we require that the ng cycles of channel training be much smaller than a single time slot or the channel coherence time. A cycle of channel training could be in the order of a few micro seconds. But the channel coherence time could be in the order of many mini seconds.

For stationary networks, the above assumption is reasonable. However, for opportunistic SAM, we also require that the channel gains change randomly from one time slot to another. For stationary network, this condition may be difficult to realize naturally. Yet, one can induce such random fluctuations of channel gains by randomly changing the phases of multiple transmitting antennas of each transmitting node. In this paper, we use the single input single output (SISO) channel model. In the case of multiple transmitting antennas, each SISO channel gain should absorb the transmitter beam vector.

The delay caused by the opportunistic SAM for each link is assumed to be tolerable.

C. Optimal Transmission Control

We show next that given a duty cycle p, the optimal form of the probabilistic control function $s(\nu)$ for any given subnet is a step function. Given $s(\nu)$ for an arbitrary subnet, the throughput of the subnet in bits-hops/s/Hz/node is now given by

$$c = \int_0^\infty c(x) s(x) f_{\nu_{0,0}}(x) dx \quad (7)$$

where $c(x) = \frac{1}{L}R_\xi Pr\{\nu_{0,0} \geq \xi(\sigma^2/P + \nu_I)|\nu_{0,0} = x\}$ with $\nu_I = \sum_{j\neq 0}\nu_{0,j}$. Here, $c(x)$ denotes the instantaneous throughput conditioned on the channel gain $\nu_{0,0} = x$, and $f_{\nu_{0,0}}(x)$ denotes the p.d.f of $\nu_{0,0}$.

Note that given the same noise power σ^2 and the same statistics of the interference ν_I from other subnets, it is obvious that the packet delivery rate $Pr\{\nu_{0,0} \geq \xi(\sigma^2/P + \nu_I)|\nu_{0,0} = x\}$ is an increasing function of x, and hence so is $c(x)$.

The optimal form of the probability function $s(\nu)$ is a solution to the following problem:

$$\begin{aligned} &\max_{s(\nu)} \int_0^\infty c(\nu)s(\nu)f_{\nu_{0,0}}(\nu)d\nu, \\ &\text{subject to} \quad p = \int_0^\infty s(\nu)f_{\nu_{0,0}}(\nu)d\nu, \\ &\text{and} \quad 0 \leq s(\nu) \leq 1 \end{aligned} \tag{8}$$

Lemma: If $f_{\nu_{0,0}}(\nu)$ is differentiable and $c(\nu)$ is a differentiable increasing function of ν, then the step function $s(\nu) = U(\nu - \theta)$ is the solution to (8) where θ satisfies $p = \int_\theta^\infty f_{\nu_{0,0}}(\nu)d\nu$.

Proof: Since both $f_{\nu_{0,0}}(\nu)$ and $c(\nu)$ are differentiable functions, (8) can be rewritten into the following discrete form with an arbitrarily small Δ:

$$\begin{aligned} &\max_{\{Q_j\}} \sum_{j=0}^\infty c_j Q_j \Delta, \\ &\text{subject to} \quad p = \sum_{j=0}^\infty Q_j \Delta, \\ &\text{and} \quad 0 \leq Q_j \leq f_j \end{aligned} \tag{9}$$

where $c_j = c(j\Delta)$, $Q_j = s_j f_j$, $s_j = s(j\Delta)$, and $f_j = f_{\nu_{0,0}}(j\Delta)$. Since c_j increases with j, the solution to (9) must be such that each Q_j takes its maximum possible value f_j for all largest values of j until the sum of these values of Q_j multiplied by Δ equals p. Equivalently, the optimal form of s_j is a step function. This simple solution is illustrated in Fig. 2. Since Δ is arbitrarily small, this solution is the same as that given in the lemma.

D. Throughput Analysis

We now derive the throughput c, in bits-hops/s/Hz/node, of the opportunistic SAM (6) under the assumption of block Rayleigh fading channels. Recall (3) that $c = \frac{1}{L}R_\xi P_d$ where L is the node population in each subnet, R_ξ the packet spectral efficiency, and P_d the probability of packet detection. The derivation of an expression of P_d is a main task in this subsection. To keep the analysis general, we will treat each subnet with a unique index.

We first write P_d into the following form (for packet reception in the subnet $\mathcal{C}_0$):

$$\begin{aligned} P_d &= Pr\left\{\nu_{0,0} \geq \xi\left(\sigma^2/P + \sum_{j\neq 0}\nu_{0,j}\right), \nu_{0,0} \geq \theta_0\right\} \\ &= Pr\left\{\sum_{j\neq 0}\nu_{0,j} \leq \frac{\nu_{0,0}}{\xi} - \frac{\sigma^2}{P}, \nu_{0,0} \geq \theta_0\right\} \end{aligned}$$

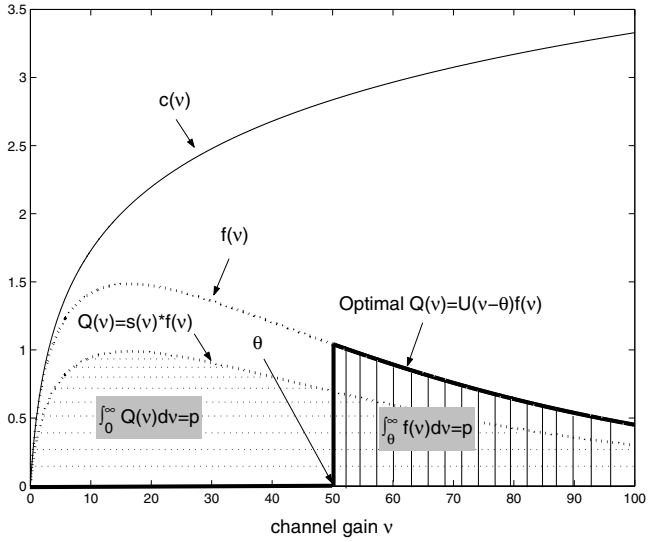

Fig. 2. Illustration of the proof of the Lemma.

$$= \int_{\max\{\xi\sigma^2/P,\theta_0\}}^\infty \int_0^{\frac{y}{\xi}-\frac{\sigma^2}{P}} f_{\nu_I}(x)dx f_{\nu_{0,0}}(y)dy \tag{10}$$

where $f_{\nu_{0,0}}(y)$ is the pdf of $\nu_{0,0}$, and $f_{\nu_I}(x)$ the pdf of $\nu_I = \sum_{j\neq 0}\nu_{0,j}$. The detailed expressions of $f_{\nu_{0,0}}(y)$ and $f_{\nu_I}(x)$ are shown next.

Since $\nu_{0,0} = \max_m \left\{|h_{0,0}(m)|^2, 1 \leq m \leq n_0\right\}$ where $|h_{0,0}(m)|^2$ is exponentially distributed with the mean $\Gamma_{0,0}(m)$, it follows that

$$\begin{aligned} Pr\{\nu_{0,0} \leq y\} &= \prod_{m=1}^{n_0} Pr\left\{|h_{0,0}(m)|^2 \leq y\right\} \\ &= \prod_{m=1}^{n_0}\left(1 - \exp\left\{-y/\Gamma_{0,0}(m)\right\}\right) \end{aligned} \tag{11}$$

Therefore,

$$\begin{aligned} f_{\nu_{0,0}}(y) &= \frac{\partial}{\partial y} Pr\{\nu_{0,0} \leq y\} \\ &= \sum_{\substack{\forall\omega_0\subseteq\Omega_0 \\ \omega_0\neq\{\phi\}}} (-1)^{|\omega_0|+1}\left(\sum_{m\in\omega_0} 1/\Gamma_{0,0}(m)\right) \\ &\quad \cdot \exp\left\{-y\sum_{m\in\omega_0} 1/\Gamma_{0,0}(m)\right\} \end{aligned} \tag{12}$$

where $\Omega_0 = \{1, 2, \ldots, n_0\}$, ω_0 denotes a subset of Ω_0, and $|\omega_0|$ the cardinality of ω_0.

To derive an expression of $f_{\nu_I}(x)$, we will use the Laplace transform (characteristic function) $\mathcal{F}_{\nu_I}(\mathcal{U})$ of $f_{\nu_I}(x)$:

$$\begin{aligned} \mathcal{F}_{\nu_I}(\mathcal{U}) &= E_{\nu_I}[e^{-\mathcal{U}\nu_I}] = E[e^{-\mathcal{U}\sum_{j=1}^S \nu_{0,j}}] \\ &= \prod_{j=1}^S E[e^{-\mathcal{U}\nu_{0,j}}] = \prod_{j=1}^S \mathcal{F}_{\nu_{0,j}}(\mathcal{U}) \end{aligned}$$

where S denotes the total number of interfering subnets, and $\mathcal{F}_{\nu_{0,j}}(\mathcal{U})$ the Laplace transform of $f_{\nu_{0,j}}(\nu)$. Based on the schedule in subnet $\mathcal{C}_j$ where $|h_{j,j}(l^*)|^2 =$

$\max_m \left\{|h_{j,j}(m)|^2, 1 \le m \le n_j\right\}$, it follows that

$$\begin{aligned} Pr\left\{\nu_{0,j} \le x\right\} &= \underbrace{Pr\left\{|h_{j,j}(l^*)|^2 < \theta_j\right\}}_{\overline{p_j}} \\ &+ \sum_{l=1}^{n_j} \underbrace{Pr\left\{l^* = l, |h_{j,j}(l)|^2 \ge \theta_j\right\}}_{p_j^l} Pr\left\{|h_{0,j}(l)|^2 \le x\right\} \\ &= \left[\overline{p_j} + \sum_{l=1}^{n_j} p_j^l \left(1 - e^{-x/\Gamma_{0,j}(l)}\right)\right] U(x) \end{aligned} \quad (13)$$

where $h_{i,j}(l)$ denotes the channel coefficient between the center node in $\mathcal{C}_i$ and the l^{th} neighboring node in $\mathcal{C}_j$ with $E\{|h_{i,j}(l)|^2\} = \Gamma_{i,j}(l)$. By definition, it follows that $\overline{p_j} = 1 - \sum_{l=1}^{n_j} p_j^l$. One can also verify that

$$\begin{aligned} \overline{p_j} &= \prod_{l=1}^{n_j} \left(1 - e^{-\theta_j/\Gamma_{j,j}(l)}\right) \\ p_j^l &= \int_{\theta_j}^{\infty} \frac{1}{\Gamma_{j,j}(l)} e^{-x/\Gamma_{j,j}(l)} \\ &\quad \cdot \prod_{k \ne l} \left(1 - e^{-x/\Gamma_{j,j}(k)}\right) dx \end{aligned} \quad (14)$$

The pdf of $\nu_{0,j}$ is the derivative of (13), i.e.

$$\begin{aligned} f_{\nu_{0,j}}(x) &= \frac{\partial}{\partial x} Pr\{\nu_{0,j} \le x\} \\ &= \overline{p_j}\delta(x) + \sum_{l=1}^{n_j} p_j^l \frac{1}{\Gamma_{0,j}(l)} e^{-x/\Gamma_{0,j}(l)} U(x) \end{aligned} \quad (15)$$

Then, it follows that

$$\begin{aligned} \mathcal{F}_{\nu_I}(\mathcal{U}) &= \prod_{j=1}^{S} \mathcal{F}_{\nu_{0,j}}(\mathcal{U}) \\ &= \prod_{j=1}^{S} \int_0^{\infty} e^{-\mathcal{U}x} f_{\nu_{0,j}}(x) dx \\ &= \prod_{j=1}^{S} \left(\overline{p_j} + \sum_{l=1}^{n_j} p_j^l \frac{1/\Gamma_{0,j}(l)}{\mathcal{U} + 1/\Gamma_{0,j}(l)}\right) \\ &= \mathcal{B} + \sum_{j=1}^{S} \sum_{l=1}^{n_j} \frac{\mathcal{A}_j^l}{\mathcal{U} + 1/\Gamma_{0,j}(l)} \end{aligned} \quad (16)$$

where $\mathcal{B} = \prod_{j \ne 0} \overline{p_j}$ and

$$\mathcal{A}_j^l = \frac{p_j^l}{\Gamma_{0,j}(l)} \prod_{k \ne 0,j} \left(\overline{p_k} + \sum_{m=1}^{n_k} p_k^m \frac{1/\Gamma_{0,k}(m)}{1/\Gamma_{0,k}(m) - 1/\Gamma_{0,j}(l)}\right)$$

The last step in (16) follows from the fractional decomposition where the roots of the common denominator are assumed to be distinct, i.e., $\Gamma_{0,j}(l) \ne \Gamma_{0,k}(m), \forall j \ne k, \forall m \ne l$. The cases of common roots would be too tedious to consider. (The above assumption of distinct roots can cause numerical problems in computations. For our numerical results shown in the next section, we added a random perturbation to the location of each node on the square grid to reduce the probability of common roots.)

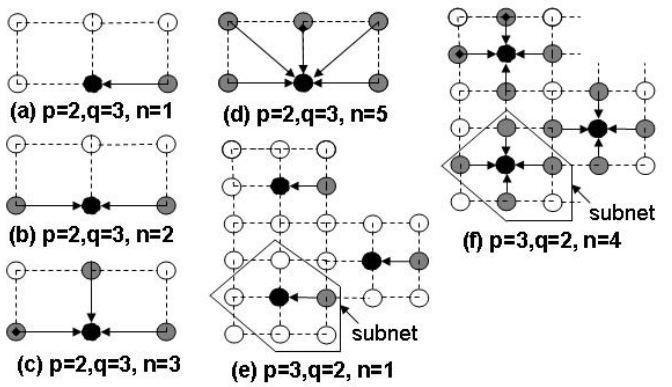

Fig. 3. Five subnets: (a) $(p, q, n) = (2, 3, 1)$; (b) $(p, q, n) = (2, 3, 2)$; (c) $(p, q, n) = (2, 3, 3)$; (d) $(p, q, n) = (2, 3, 5)$; (e) $(p, q, n) = (3, 2, 1)$; (f) $(p, q, n) = (3, 2, 4)$.

Taking the inverse Laplace transform of (16), we have the pdf of ν_I:

$$\begin{aligned} f_{\nu_I}(x) &= \mathcal{L}^{-1}\left\{\mathcal{F}_{\nu_I}(\mathcal{U})\right\} \\ &= \mathcal{B}\delta(x) + \sum_{j=1}^{S} \sum_{l=1}^{n_j} \mathcal{A}_j^l \exp\{-x/\Gamma_{0,j}(l)\} \end{aligned} \quad (17)$$

Since $\int_0^{\infty} f_x(\nu) dx = 1$, it holds that $\mathcal{B} + \sum_{j=1}^{S} \sum_l \mathcal{A}_j^l \Gamma_{0,j}(l) = 1$. Also note that if $\theta_j = 0, \forall j \ne 0$, then $\mathcal{B} = 0$.

Since both $f_{\nu_{0,0}}(y)$ and $f_{\nu_I}(x)$ are exponential functions, it is straightforward (although with some work) to verify from (10), (12) and (17) that P_d is given by (18) where $\mu_{i,j}(l) = 1/\Gamma_{i,j}(l)$.

Note that for a uniform network, both n_j and θ_j used in this subsection should be independent of j. For the multiuser SAM, switching SAM and deterministic SAM, the corresponding expression of P_d can be obtained from (18) by setting the values of n and θ properly.

IV. A Case Study

To illustrate the throughput of the opportunistic SAM, we now focus on a large network on a square grid as shown in Fig. 1. During each time slot of the opportunistic SAM, the network can be viewed as a set of contiguous subnets. Each subnet has a center (receiving) node, n active neighboring nodes and $L - n - 1$ idle neighboring nodes. The size of each subnet is governed by the vertical spacing p of adjacent center nodes and the horizontal spacing q of adjacent center nodes. It follows that $L = pq$. In Fig. 1, $(p, q) = (2, 3)$. Note that (p, q) is not equivalent to (q, p). This is because p is the vertical spacing between two adjacent center nodes that are aligned vertically while q is the horizontal spacing between two adjacent center nodes that are not aligned horizontally. For convenience, we assume that the distance between adjacent nodes is $d = 1$ meter. For other values of d, the discussions to be shown also apply if the corresponding power P is replaced by P/d^{α} where α is the path loss exponent. We will choose $\alpha = 4$ in the following discussions.

$$P_d = 1 - \prod_{m=1}^{n_0} \left(1 - e^{-\max\{\frac{\sigma^2\xi}{P},\theta\}\mu_{0,0}(m)}\right) - \sum_{j=1}^{S}\sum_{l=1}^{n_j} \frac{\mathcal{A}_j^l e^{-\left(\max\{\frac{\sigma^2}{P},\frac{\theta}{\xi}\}-\frac{\sigma^2}{P}\right)\mu_{0,j}(l)}}{\mu_{0,j}(l)} \left(\sum_{\substack{\forall \omega_0 \subseteq \Omega_0 \\ \omega_0 \neq \{\phi\}}} \frac{(-1)^{|\omega_0|+1} \sum_{m\in\omega_0} \mu_{0,0}(m)}{\sum_{m\in\omega_0} \mu_{0,0}(m) + \frac{\mu_{0,j}(l)}{\xi}} e^{-\max\{\frac{\sigma^2\xi}{P},\theta\} \sum_{m\in\omega_0} \mu_{0,0}(m)} \right) \quad (18)$$

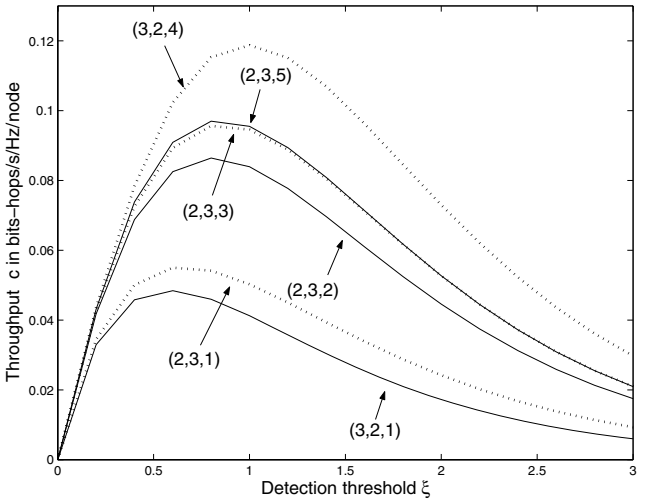

Fig. 4. Throughput comparison under $\theta = 0$ and $\frac{P}{\sigma^2} = 0dB$.

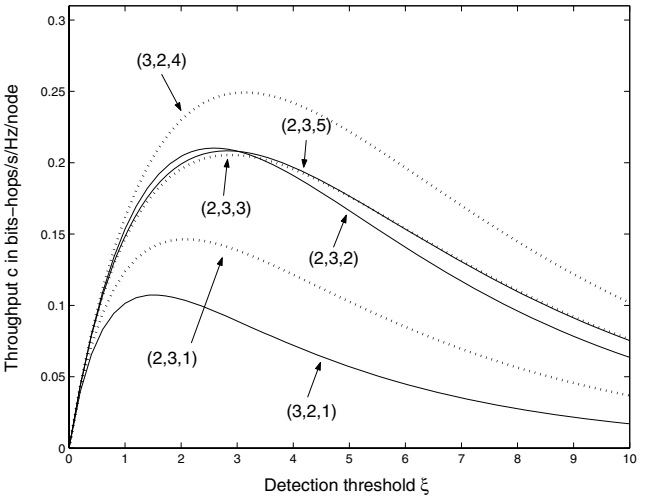

Fig. 5. Throughput comparison under $\theta = 0$ and $\frac{P}{\sigma^2} = 10dB$.

Each subnet is governed by the three integers (p, q, n). In Fig. 3, four subnets (a), (b), (c) and (d), corresponding to $(p, q, n) = (2, 3, 1), (2, 3, 2), (2, 3, 3), (2, 3, 5)$, are respectively illustrated. Also shown in Fig. 3 are two subnets (e) and (f), corresponding to $(p, q, n) = (3, 2, 1), (3, 2, 4)$, respectively. Based on our computations, choices other than $(p, q) = (2, 3)$ and $(p, q) = (3, 2)$ lead to significantly smaller network throughput in bits-hops/s/Hz/node. Therefore, those values other than $(p, q) = (2, 3)$ and $(p, q) = (3, 2)$ will not be discussed. Also note that for both $(p, q) = (2, 3)$ and $(p, q) = (3, 2)$, the product pq is the same.

A. *Effect of* n

The effect of $n > 1$ on the network throughput is illustrated by Figures 4, 5 and 6, where P/σ^2 is the nominal signal-to-noise ratio (SNR) and ξ is the detection SINR threshold. The three figures correspond to $P/\sigma^2 = 0dB$, $P/\sigma^2 = 10dB$ and $P/\sigma^2 = 50dB$, respectively.

In all these figures, the transmission threshold θ on each local channel gain is set to $\theta = 0$. Therefore, each curve in these figures corresponds to either the deterministic SAM (with $n = 1$) or the multiuser SAM (with $n > 1$). From these figures, we can make the following observations:

First, for the deterministic SAM, $(p, q) = (2, 3)$ is better than $(p, q) = (3, 2)$. This is consistent with the non-fading channel results shown in [1]. (A more detailed analysis of the deterministic SAM for non-square topologies is available in [6] and [7].)

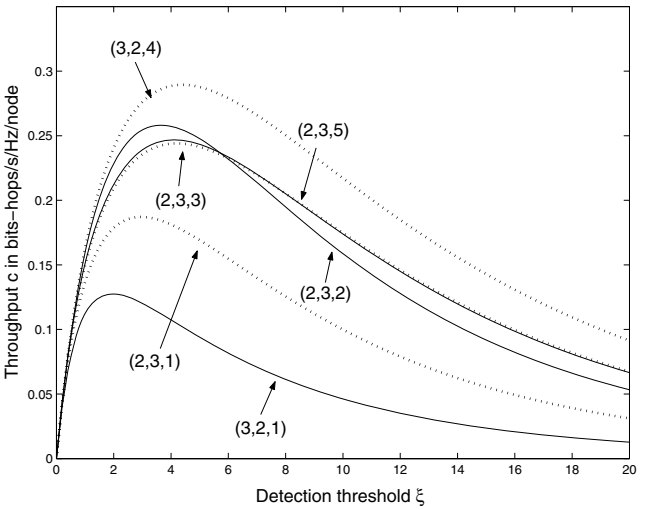

Fig. 6. Throughput comparison under $\theta = 0$ and $\frac{P}{\sigma^2} = 50dB$.

Second, when P/σ^2 is high and ξ is low, $(p, q, n) = (2, 3, 2)$ may yield a higher throughput than $(p, q, n) = (2, 3, 3)$. This is because under $(p, q, n) = (2, 3, 3)$, the active node just above its center node is located immediately next to the center node in another subnet, which causes a high interference when P/σ^2 is high and ξ is low.

Third, between the two choices $(p, q, n) = (2, 3, 3)$ and $(p, q, n) = (2, 3, 5)$, the difference in network throughput is small. This is because under $(p, q, n) = (2, 3, 5)$, the two

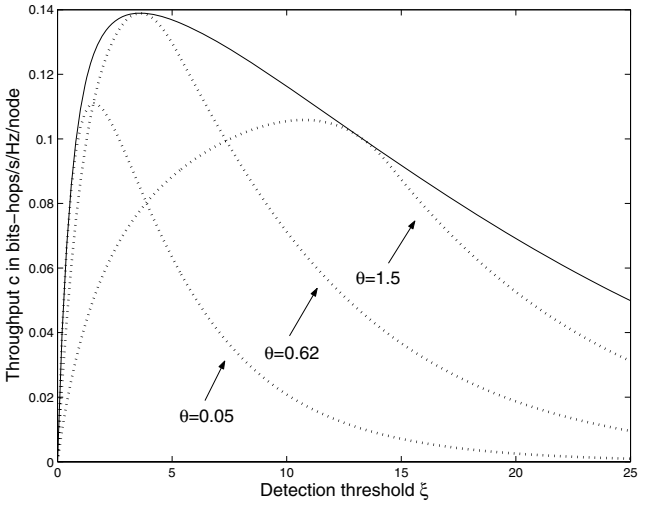

Fig. 7. Throughput for various θ under $(p,q,n)=(3,2,1)$ and $\frac{P}{\sigma^2}=10dB$.

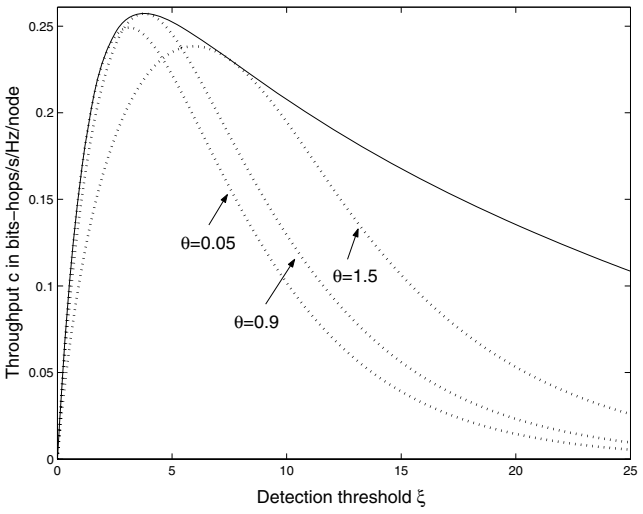

Fig. 8. Throughput for various θ under $(p,q,n)=(3,2,4)$ and $\frac{P}{\sigma^2}=10dB$.

active nodes at the corners are farther away from their center node than the other three active nodes. With the factor $\sqrt{2}$ on the distance for the two corner nodes, the Rayleigh fading and the path loss exponent $\alpha=4$, it can be shown that the probability for one of the two corner nodes to have a larger channel gain (with respect to their center node) than the other three nodes is only about 5%. This explains why $(p,q,n)=(2,3,3)$ and $(p,q,n)=(2,3,5)$ have essentially the same throughput.

Fourth, under $(p,q,n)=(3,2,4)$, the center node of each subnet has four equal-distance neighbors, instead of three under $(p,q,n)=(2,3,3)$. Furthermore, under $(p,q,n)=(3,2,4)$, the shortest distance between an active node in one subnet and the center node in another subnet is $\sqrt{2}$, instead of 1 under $(p,q,n)=(2,3,3)$. This explains why the throughput under $(p,q,n)=(3,2,4)$ is the highest among all cases considered in these figures.

B. Effect of θ

The effect of $\theta>0$ is illustrated in Fig. 7 where $(p,q,n)=(3,2,1)$ and $P/\sigma^2=10dB$ and also in Fig. 8 where $(p,q,n)=(3,2,4)$ and $P/\sigma^2=10dB$. In each figure, three dash-line curves with fixed values of θ are shown, and also shown is a solid-line curve corresponding to the optimal θ at any ξ. These figures indicate the importance of the optimal choice of θ at each ξ.

C. Optimal θ versus ξ

The optimal θ versus ξ is illustrated in Fig. 9 where $P/\sigma^2=0dB$ and $P/\sigma^2=10dB$, and also in Fig. 10 where $P/\sigma^2=50dB$.

For each choice of P/σ^2, the four subnets $(p,q,n)=(2,3,1),(2,3,3),(3,2,1),(3,2,4)$ are considered. We see that at $P/\sigma^2=0dB$, the relationship between the optimal θ and the choice of ξ is basically linear. In fact, it is easy to show that if either P/σ^2 is low or ξ is high, then $\theta_{opt}=\xi\frac{\sigma^2}{P}$. Indeed, if P/σ^2 is low, then the interference is negligible comparing to noise and hence the optimal θ on the local channel gain ν

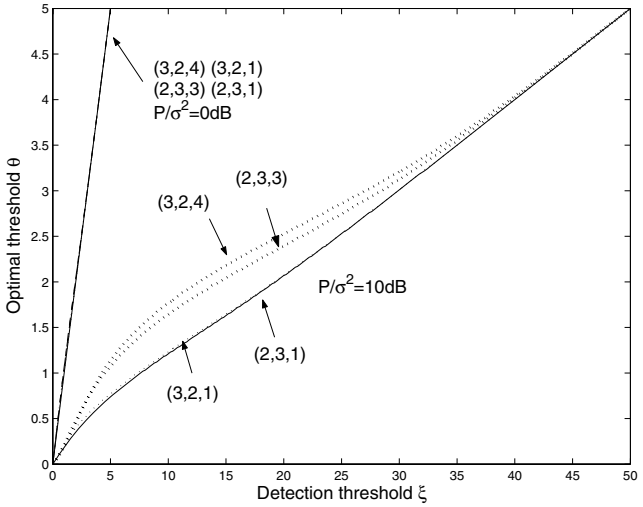

Fig. 9. Optimal θ versus ξ for $\frac{P}{\sigma^2}=0dB$ and $\frac{P}{\sigma^2}=10dB$ under $(p,q,n)=(2,3,1),(2,3,3),(3,2,1),(3,2,4)$.

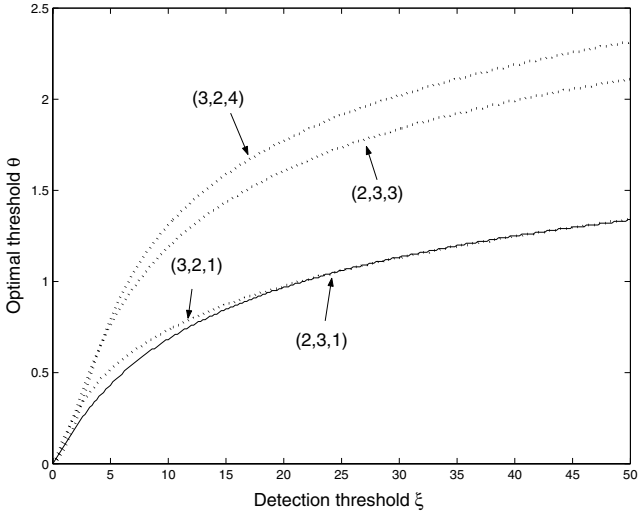

Fig. 10. Optimal θ versus ξ for $\frac{P}{\sigma^2}=50dB$ under $(p,q,n)=(2,3,1),(2,3,3),(3,2,1),(3,2,4)$.

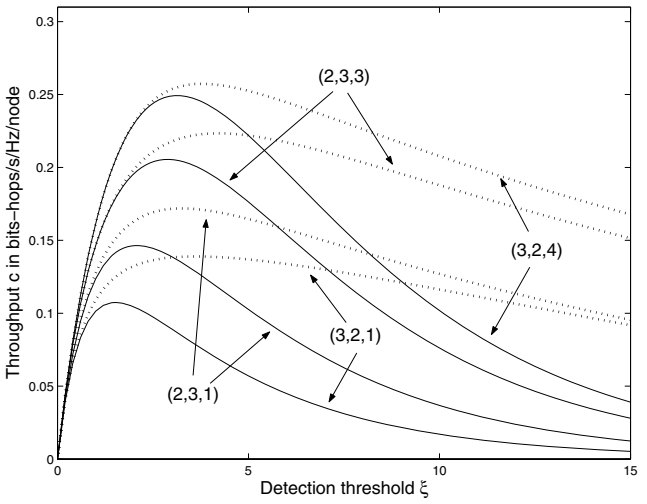

Fig. 11. Comparison of throughput between $\theta = 0$ (solid-line) and $\theta = \theta_{opt}$ (dash-line) for $\frac{P}{\sigma^2} = 10dB$ under $(p, q, n) = (2, 3, 1), (2, 3, 3), (3, 2, 1), (3, 2, 4)$.

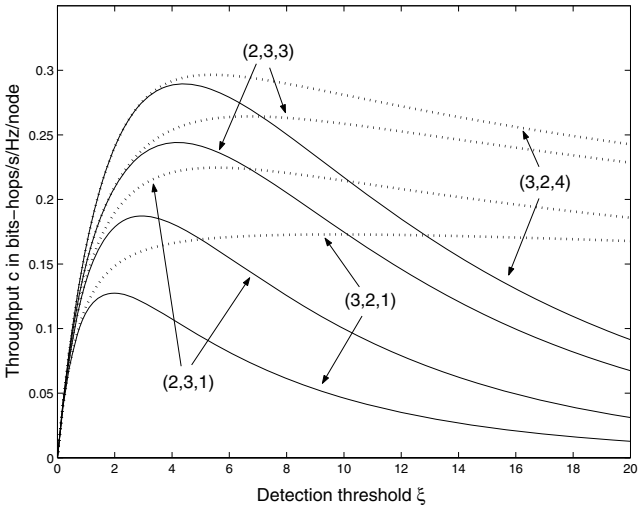

Fig. 12. Comparison of throughput between $\theta = 0$ (solid-line) and $\theta = \theta_{opt}$ (dash-line) for $\frac{P}{\sigma^2} = 50dB$ under $(p, q, n) = (2, 3, 1), (2, 3, 3), (3, 2, 1), (3, 2, 4)$.

should be such that $P\theta_{opt}/\sigma^2 = \xi$, i.e., $\theta_{opt} = \xi\frac{\sigma^2}{P}$. On the other hand, if ξ is high, then with a high probability the local channel gain cannot meet the required threshold for successful packet detection and hence with a high probability there is no transmis sion in any given subnet. In this case, there is little interference in the network, and hence the optimal θ is still given by $\theta_{opt} = \xi\frac{\sigma^2}{P}$.

In general, it is obvious that $\theta_{opt} \geq \xi\frac{\sigma^2}{P}$. The more interference there is, the more deviated is θ_{opt} from $\xi\frac{\sigma^2}{P}$. Fig. 9 and Fig. 10 support this conclusion. It is also important to note here that for maximal network throughput, P/σ^2 should be chosen as large as possible. In this case, θ_{opt} should significantly deviate from $\xi\frac{\sigma^2}{P}$.

D. Effect of Optimal θ

In each of Fig. 11 (where $P/\sigma^2 = 10dB$) and Fig. 12 (where $P/\sigma^2 = 50dB$), we compare the throughput between $\theta = 0$ and $\theta = \theta_{opt}$ under $(p, q, n) = (2, 3, 1), (2, 3, 3), (3, 2, 1), (3, 2, 4)$.

The dash-line curves are for $\theta = \theta_{opt}$, and the solid-line curves are for $\theta = 0$. We see that for small n (i.e., $n = 1$) the peak throughput is increased significantly by using optimal θ. We also see that if n is large (i.e., $n = 3$ or $n = 4$) then the optimal θ does not yield a major increase in peak throughput but provides a robustness of the throughput versus ξ.

Finally, it is important to note that by further increasing P/σ^2, the network throughput stays about the same. Fig. 12 essentially shows the maximum possible throughput under the opportunistic SAM.

V. Conclusion

In this paper, we have introduced a distributed medium access control (MAC) scheme called opportunistic synchronous array method (opportunistic SAM) for a large network of wireless routers. We assume that the network is relatively stationary so that the estimation of channel responses only causes a relatively minor overhead. We also assume that the channel responses change randomly over a time scale much larger than the time spent for channel estimation. We have provided an analysis of the intra-network throughput (as opposed to inter-network throughput via gateways) of the opportunistic SAM under a uniform traffic demand. This statistical analysis is based on many channel coherence intervals. The results have shown that the opportunistic SAM yields a significant improvement in network throughput over non-opportunistic SAM.

SAM is a topology dependent MAC scheme. There are topology independent MAC schemes such as ALOHA and CSMA [12]. But the network throughput of these schemes is known to be lower than that of SAM. For a throughput comparison between SAM and ALOHA, see [6]. CSMA causes a large sparseness between concurrent co-channel transmissions, and such a large sparseness is known to cause a much reduced network throughput [1], [6].

For the throughput analysis in this paper, the traffic loading is assumed to be uniform. For non-uniform traffic, the opportunistic SAM can be integrated with the fairness mechanism proposed in Section 3.1. But a thorough analysis of its convergence behavior remains an important task for future research.

References

[1] Y. Hua, Y. Huang, and J. J. Garcia-Luna-Aceves, "Maximizing the throughput of large ad hoc wireless networks," *IEEE Signal Processing Mag.*, vol. 23, pp. 84–94, Sept. 2006.

[2] P. Gupta and P. R. Kumar, "The capacity of wireless networks," *IEEE Trans. Inform. Theory*, vol. 46, no. 2, pp. 388–404, Mar. 2000.

[3] L.-L. Xie and P. R. Kumar, "A network information theory for wireless communication: scaling laws and optimal operation," *IEEE Trans. Inform. Theory*, vol. 50, no. 5, pp. 748–767, May 2004.

[4] F. Xue, L.-L. Xie, and P. R. Kumar, "The transport capacity of wireless networks over fading channels," *IEEE Trans. Inform. Theory*, vol. 51, no. 3, pp. 834–847, Mar. 2005.

[5] X. Liu and M. Haenggi, "Throughput analysis of fading sensor networks with regular and random topologies," *EURASIP J. Wireless Commun. and Networking*, pp. 554–564, 2005.

[6] K. Hong and Y. Hua, "Throughput of large wireless networks on square, hexagonal, and triangular grids," in *Proc. IEEE Workshop on Sensor Array and Multi-channel Processing*, Waltham, MA, July 2006, pp. 462–466.

[7] ——, "Throughput analysis of large wirelss networks with regular topologies," *EURASIP J. Wireless Commun. and Networking*, vol. 2007, 2007, article ID 26760, 11 pages.

[8] R. Knopp and P. A. Humblet, "Information capacity and power control in single-cell multiuser communications," in *Proc. IEEE Int. Conf. on Commun. (ICC)*, June 1995.

[9] P. Viswanath, D. Tse, and R. Laroia, "Opportunistic beamforming using dumb antennas," *IEEE Trans. Inform. Theory*, vol. 48, pp. 1277–1294, June 2002.

[10] X. Qin and R. Berry, "Exploiting multiuser diversity for medium access control in wireless networks," in *Proc. IEEE INFOCOM*, Mar. 2003.

[11] S. Adireddy and L. Tong, "Exploiting decentralized channel state information for random access," *IEEE Trans. Inform. Theory*, vol. 51, pp. 537–561, Feb. 2005.

[12] G. Bianchi, "Performance analysis of the IEEE 802.11 distributed coordination function," *IEEE J. Select. Areas Commun.*, vol. 18, no. 3, pp. 535–547, Mar. 2000.

Bin Zhao received the B.S.E.E. and M.S.E.E. degrees from Shanghai Jiaotong University, Shanghai, China, in 1995 and 1998 respectively. He received a Ph.D. degree in electrical engineering from West Virginia University (Morgantown, WVa, U.S.A.) in 2004, where he worked as a research assistant in the Wireless Communications Research Laboratory. He is currently a senior engineer and digital communications specialist with Cinea Inc, a wholly owned subsidiary of Dolby Laboratory Inc. His research interests are in the areas of communications theory, error-correction coding, sensor networking, and information theory. Prior to joining Cinea Inc, he was a DSP Engineer with Huawei Technologies Co. Ltd. from Sep. 1997 to July 1999, a Communications Engineer with Efficient Channel Coding Inc. (now ViaSat Inc.) from July 2004 to Dec. 2005, and a Posdoc Research Fellow with University of California, Riverside, Department of Electrical Engineering from Dec 2005 to May 2007.

Yingbo Hua (S'86-M'88-SM'92-F'02) received B.E. degree in Feb 1982 from Nanjing Institute of Technology (Southeast University), Nanjing, China, and M.S. degree in 1983 and Ph.D. degree in 1988 from Syracuse University, Syracuse, NY. He was supported by Chinese Government Scholarship and Syracuse University Graduate Fellowship.

In Feb 1990, he joined the faculty of the University of Melbourne, Melbourne, Australia, where he stayed until 2001. Since Feb 2001, he has been Professor of Electrical Engineering with the University of California, Riverside, CA. He has published over 260 articles in journals, conference proceedings and books in areas such as sensor array and high-resolution signal processing, principal component analysis and reduced rank filtering, blind system identification and source separations, cooperative wireless relay networks, and throughput enhancement for large-scale wireless networks.

He co-edited two books and has served on Editorial Boards of *IEEE Transactions on Signal Processing*, *IEEE Signal Processing Letters*, *Signal Processing (EURASIP)* and *IEEE Signal Processing Magazine*. He has also served as Guest Editor for two *IEEE Signal Processing Magazine* Special Issues.

He was a member on IEEE Signal Processing Society's Technical Committees for Underwater Acoustic Signal Processing, Sensor Array and Multi-Channel Signal Processing, and Signal Processing for Communications and Networking. He has served on numerous technical program committees of international conferences and workshops. He is a Fellow of IEEE.